

Current Status of Simulation for the Tau Air-Shower Mountain-Based Observatory

Jeffrey Lazar* and **Pavel Zhelnin** for the TAMBO collaboration

E-mail: jlazar@icecube.wisc.edu, pzhelnin@g.harvard.edu

While IceCube's detection astrophysical neutrinos at energies up to a few PeV has opened a new window to our Universe, much remains to be discovered regarding these neutrinos' origin and nature. In particular, the difficulty differentiating ν_e and ν_τ charged-current (CC) events in the energy limits our ability to measure precisely the flavor ratio of this flux. The Tau Air-Shower Mountain-Based Observatory (TAMBO) is a next-generation neutrino observatory capable of producing a high-purity sample of ν_τ CC events in the energy range from 1-100 PeV, i.e. just above the IceCube measurements. An array of water Cherenkov tanks and plastic scintillators deployed on one face of the Colca Canyon will observe the air-shower produced when a τ lepton, produced in a ν_τ CC interaction, emerges from the opposite face and decays in the air. In this contribution, I will present the current status of the TAMBO simulation, including preliminary sensitivities to various flux models.

38th International Cosmic Ray Conference (ICRC2023)
26 July - 3 August, 2023
Nagoya, Japan



*Speaker

1. Introduction

Since IceCube’s discovery of a diffuse astrophysical flux in 2013, the field of neutrino astronomy has taken immense stride. This year, IceCube has announced the observation neutrinos from the Galactic Plane [1] and of high-significance neutrino point sources [2]. Among the outstanding goals of this field is the characterization of the diffuse flux, both in terms of its high-energy spectral shape and its flavor composition. IceCube has measured this flux in the energy range from tens of TeV up to a few PeV; however, the spectrum remains unknown at higher energy. Some models predict a spectral cutoff around 6 PeV, stressing the importance of measuring the flux in the energy range just above IceCube’s observations. Furthermore, this energy range is important for measuring the flavor composition of the flux, since for most of the energies to which IceCube is sensitive, events produced by tau neutrinos are indistinguishable from those produced by electron neutrinos.

TAMBO, the Tau Air Shower Mountain-Based Observatory, is a planned next-generation, deep-valley neutrino telescope designed to be sensitive to tau neutrinos with energies ranging from 1–100 PeV. This experiment will bridge the gap between high-energy and planned ultra-high-energy neutrino telescopes. Additionally, TAMBO will play a key role in neutrino flavor ratio measurements, as the observatory is fundamentally designed to distinguish tau neutrinos from other neutrino flavors. The detector is planned to be an array of plastic scintillator panel or water Cherenkov tanks deployed on the side of the Colca Valley in the Peruvian Andes mountain range. These will detect secondary particles created from a charged tau lepton decaying and causing an extensive air shower.

Although the event rate and effective area of TAMBO was estimated in a previous work [3], a detailed simulation had not been performed. In this proceeding, we will describe the status of the TAMBO simulation framework. This pipeline uses the Julia [4] programming language to interface with the existing TauRunner [5], PROPOSAL [6], and CORSIKA [7] to propagate high-energy tau neutrinos, charged tau leptons, and extensive air showers, respectively. Additionally, it includes newly implemented injection and weighting protocols written entirely in Julia.

2. Event Injection

The first step in the simulation is choosing the initial neutrino properties, *e.g.* energy, propagation direction, and interaction vertex. This process, known as event injection, requires balancing the desire to simulate all neutrinos that could possibly trigger the detector with the need to maintain computational efficiency. In this section, we will describe the approach we take to achieving this balance, which is inspired by the approach in Ref. [8].

Before we can describe the injection computation; however, we must first define the environment in which the simulation is to take place. This region, called this the simulation volume, is the region of the Peruvian Colca Valley centered at coordinates $(-15.581^\circ, -72.12^\circ)$, extending 22.1 km to the east and west and 17.7 km north and south. Furthermore, this region extends to 7.5 km above sea level and 17.5 km underground. The location and size of this region were selected so as to contain all sites of interest for the TAMBO detector, as well as to have sufficient padding so that all neutrino interactions that could trigger the detector. For the purposes of our current simulation, we have placed the center of the detector at coordinates $(-15.67^\circ, -72.16^\circ)$, *i.e.* in the

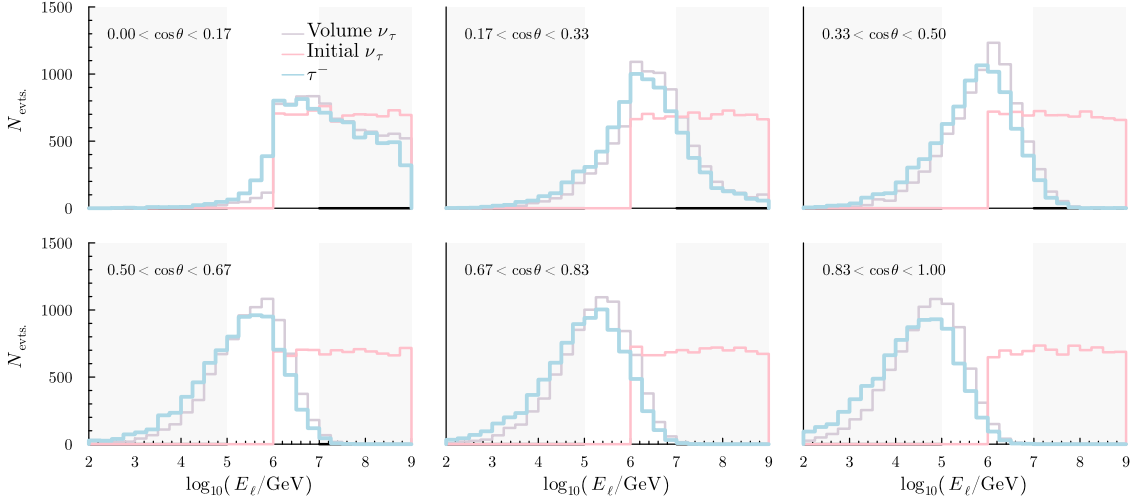


Figure 1: Lepton energies at different injection stages as a function of angle. All events are drawn from a power law with a spectral index of 1, as evidenced by the pink line being flat in each panel. As we move from Earth-skimming neutrinos in the top, left panel to core-traversing neutrinos in the bottom, right panel, the distribution of energies at the TAMBO simulation volume moves to lower energies due to tau regeneration; however, the total number of events is conserved. The distribution is further shifted to lower energies when the tau neutrino creates a charged tau lepton. This effect is less pronounced for higher-energy neutrinos since the charged-current interaction becomes more elastic. The shaded regions roughly correspond to the energy range to which TAMBO is sensitive. Only angles shown in the top row of panels were considered in previous sensitivity estimates. Clearly, steeper angles contribute to the total number of neutrino interactions near the detector; however, further study is required to know if these events will trigger the detector.

southwestern quadrant of the simulation region. This corresponds to a large, flat expanse of the canyon, well-suited to detector deployment.

Having defined a detector position and local environment, we can now inject events. We begin by sampling the direction of the neutrinos momentum. We sample this uniformly on a unit sphere by drawing the zenith angle, θ , uniformly in $\cos \theta$ and the azimuthal angle, ϕ uniformly in ϕ . We then pick a point of closest approach by sampling a point on a disc, centered at TAMBO's center, the normal vector of which is parallel to the neutrino momentum. The radius of this disc, r_{inj} , should contain the detector; in this work, we set it to 2 km, but this may be changed in the future. We can then backtrace the direction of the neutrino and determine whether it had to cross the Earth in order to arrive at TAMBO.

Next, we must determine the energy of the neutrino when it enters the simulation region. If the neutrino did not have to traverse the Earth, we may draw an energy from a power-law distribution and set this equal to the energy of the neutrino at the edge of the simulation region. If the neutrino had to cross a portion of the Earth, we sample an energy from the same power-law distribution and set this equal to the energy of the neutrino at the surface of the Earth and propagate the neutrino to the detector. At the energies that TAMBO can probe, tau regeneration [9] plays a crucial role in the tau-neutrino propagation. To simulate this, we interface to the Python-based TauRunner package [5]. This package uses Monte Carlo methods to propagate neutrinos with energies between 10 GeV and 10^{12} GeV, accounting for secondary neutrinos produced in charged-current tau neutrino

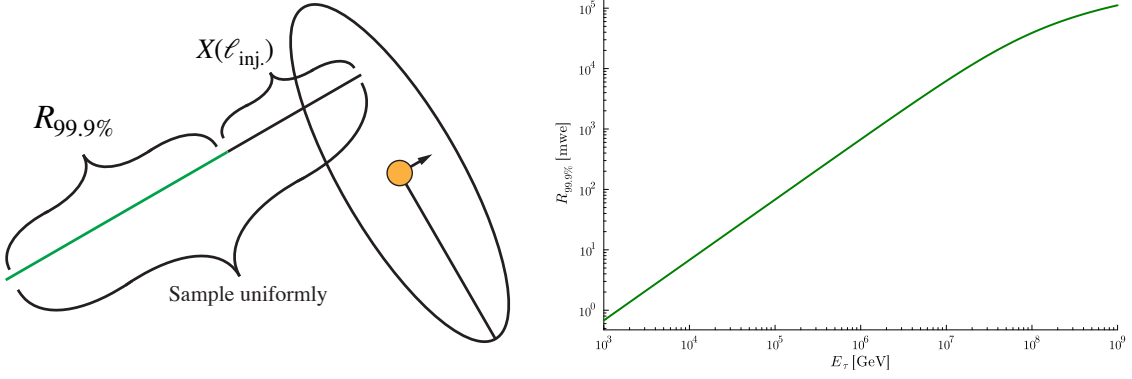


Figure 2: Diagram of ranged vertex sampling procedure. The so-called injection disc—the large black ring—is centered on the center of the detector, represented here as an orange circle and is oriented perpendicular to the direction of the incident neutrino direction. An interaction vertex is sampled by computing $R_{99.9\%}$ —shown in the plot on the right—for the exiting charged tau lepton and sampling a distance in the range $[0, \ell_{\text{inj.}} + \ell(R_{99.9\%}|\theta, \phi)]$ uniformly in column depth.

interactions and treating charged tau energy losses stochastically. Although there are a variety of packages that specialize in treating tau regeneration, *TauRunner* is one of two—the other being *NuPropEarth* [10]—that gives the tau neutrino flux. As such, only these two software are suitable for event injection; however, we opt for *TauRunner* since its Python implementation is easier to interface with from Julia. Once *TauRunner* has propagated the neutrino to the surface of the simulation volume, we set the final neutrino energy from *TauRunner* to the energy in the simulation volume.

We now know the energy of the neutrino that we will force to undergo a charged-current interaction, and as such can sample the outgoing charged tau lepton energy. To do this, we sample from the differential cross section as computed by Cooper-Sarkar, Mertsch, and Sarkar [11] and as implemented in [12]. We assume that the momentum of the outgoing tau lepton is parallel to that of the neutrino, and as such we only need to sample from the Bjorken- y distribution. The process of the energy treatment, from initial neutrino, to propagation to the simulation region, to final charged tau lepton energy can be seen in Fig. 1

At last, we can sample an interaction vertex and thus conclude the event injection. We must make sure that we are sampling all vertices that could lead to the air-shower from the charged tau lepton to trigger the detector. Since higher-energy tau leptons can travel for larger distances before decaying, this process should depend on energy. We solve this by computing $R_{99.9\%}(E_\tau)$, the 99.9% quantile of distances τ leptons can travel before decaying. This is computed for a number of energies, and is then fit to the parametrization:

$$R_{99.9\%}(E_\tau) = \frac{1}{\beta} \log \left[1 + E_\tau \frac{\beta}{\alpha} \right].$$

After propagating 10^5 tau leptons at energies ranging from 10^3 GeV to 10^8 GeV with the PROPOSAL software [6], we found best-fit values of $\alpha = 1.473 \times 10^3$ GeV mwe $^{-1}$ and $\beta = 2.63 \times 10^{-5}$ mwe $^{-1}$. We then sample a distance from the point of closest approach in the range $d \in [0, \ell_{\text{inj.}} + \ell(R_{99.9\%}|\theta, \phi)]$, where $\ell_{\text{inj.}}$ is an injection parameter and $\ell(X|\theta, \phi)$ a function that converts a column depth to a

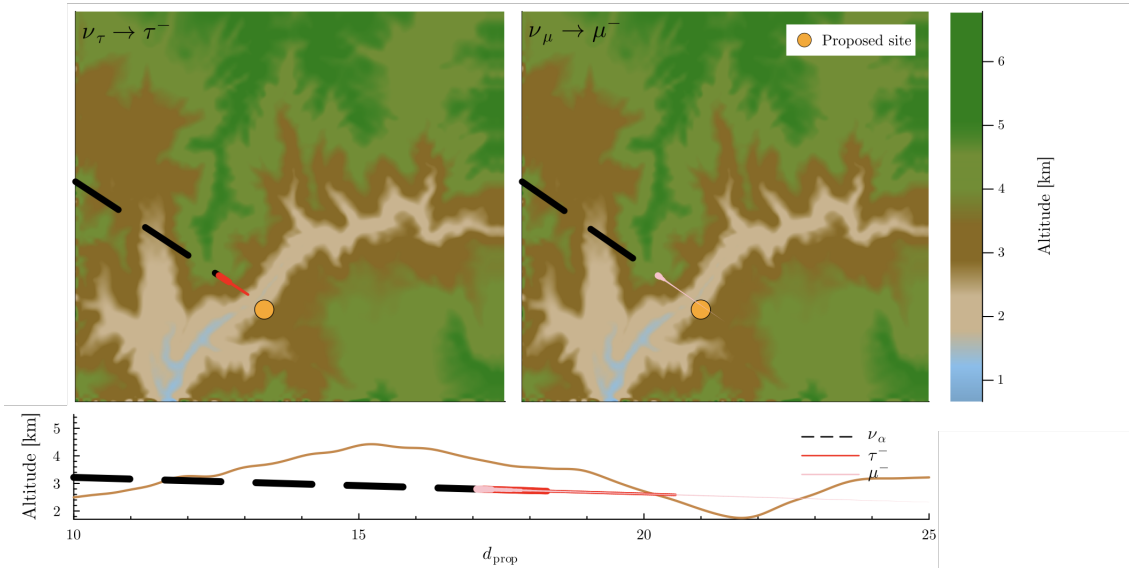


Figure 3: Propagation process for tau and mu neutrinos. The top panels show a bird-eye view of the propagation process, while the bottom panel shows the process from a vantage point perpendicular to the neutrino momentum. The thickness of the line in each plot is proportional to the energy of the lepton. Since the simulation does not differentiate between neutrino flavors within the simulation region, we represent the neutrino as a dashed black line in both cases. Once a charged-current interaction takes place, we simulate the energy losses of the particle in matter. As mentioned in the main text, the charged mu lepton loses energy much more quickly than the charged tau lepton, and does not decay as promptly.

distance, is sampled uniformly in column depth. We then set the interaction vertex a distance d from the point of closest approach, in the direction opposite the neutrino momentum.

3. Final State Propagation

3.1 Charged Lepton Propagation with PROPOSAL

Once the initial quantities have been set, the outgoing charged tau lepton is propagated through the simulation volume until decay using the PROPOSAL software. This software, which uses Monte Carlo techniques to simulate the passage of charged leptons through matter, contains up-to-date cross sections for ionization, bremsstrahlung, photonuclear interactions, electron pair production, Landau–Pomeranchuk–Migdal and Ter-Mikaelian effects, muon and tau decay, as well as Molière scattering. Furthermore, it has been widely used, and as such has been well-tested by the community.

In Fig. 3, the full path an event takes from entering the simulation region to either decaying or coming to rest for two different incident neutrino types. As can be seen on the left-hand plot, the charged tau lepton which emerges from the a tau neutrino charged-current interaction retains most of its energy and decays quickly in the valley. If we exchange the incident tau neutrino for an incident muon neutrino, the story is quite different. Although the interaction vertex is the same in each case, the emerging charged mu lepton is too long-lived and does not decay in the valley, and thus cannot create an air-shower for TAMBO to detect. Furthermore, even if the muon did decay

quickly enough, it loses energy very quickly in the mountain, and thus its air shower would be more difficult for TAMBO to detect than that of an air-shower.

3.2 Air-Shower Simulation with CORSIKA

After allowing the charged tau lepton to decay in PROPOSAL, we gather the decay products, and move to simulating the air shower. To model the extensive air showers (EAS) from tau decays we use CORSIKA8, an updated C++/Python version of the FORTRAN-based CORSIKA7. To begin simulating air showers, we take tau decay products from PROPOSAL, which propagates taus until decay, and given energy, direction, interception plane orientation, and local geography we simulate an air shower. If there is an obstruction, like a mountainside, in that path of an air shower's shower axis then that event is cut. Other cuts include, a max elevation limit on how far above the valley-side will we accept air showers to be propagated, a max distance limit on shower length, cutting showers that are initiated in rock, and any down-going showers. Furthermore we track all particles from an air shower unless they fall below 1 GeV.

4. Event Weighting

In order to determine the rate of events at the detector, we must undo all unphysical choices that were made in the simulation chain, a process known as event weighting. Since TauRunner, PROPOSAL, and CORSIKA simulate according to physical processes, we need only be concerned with removing unphysical choices from event injection. Again drawing inspiration from [8], we define the probability of generating an event according to our injection procedure as:

$$p_{\text{gen.}} = \frac{1}{A_{\text{inj.}} \Omega_{\text{inj.}}} \frac{\rho(\vec{x}_{\text{int.}})}{X_{\text{gen.}}} \frac{1}{\sigma(E_{\nu}^{\text{vol.}})} \frac{\partial \sigma}{\partial y}(E_{\ell} | E_{\nu}) \frac{\Phi(E_{\nu}^{\text{gen.}})}{\int_{E_{\text{min.}}}^{E_{\text{max.}}} dE_{\nu} \Phi(E_{\nu})}.$$

Where $A_{\text{inj.}}$ is the area of the injection disc, $\Omega_{\text{inj.}}$ is the solid angle of the directional sampling, $\rho(\vec{x}_{\text{int.}})$ is the mass density evaluated at the interaction vertex, $X_{\text{gen.}}$ is the total column depth in the range $[0, \ell_{\text{inj.}} + \ell(R_{99.9\%}|\theta, \phi)]$, $\sigma(E_{\nu}^{\text{vol.}})$ is the total neutrino cross section evaluated at the neutrino energy when it enters the simulation volume, $\frac{\partial \sigma}{\partial y}(E_{\ell} | E_{\nu})$ is the differential cross neutrino cross section, Φ is the power-law spectrum according to which the initial, *i.e.* at the surface, neutrino energies were drawn from, and $E_{\text{min.}}$ and $E_{\text{max.}}$ are the minimum and maximum energies that can be sampled. It should be noted that all quantities with inj. are metaparameters of a given injection and do not vary from event to event.

The true rate of a physical event may be computed with:

$$\Gamma_{\text{evt.}} = \frac{1}{p_{\text{gen.}}} \frac{X_{\text{phys.}} N_A}{M_{\text{iso.}}} \frac{\rho_{\text{phys.}}(\vec{x}_{\text{int.}})}{X_{\text{phys.}}} \frac{\partial \sigma}{\partial y}(E_{\ell} | E_{\nu}) \Phi_{\text{phys.}}(E_{\nu}^{\text{gen.}}),$$

where $X_{\text{phys.}}$ is the column depth traversed by the neutrino en route to the interaction vertex, N_A is Avogadro's number, $M_{\text{iso.}}$ is the isoscalar nucleon mass, $\rho_{\text{phys.}}(\vec{x}_{\text{int.}})$ is the mass density of the physical medium evaluated at the interaction vertex, and $\Phi_{\text{phys.}}$ is the physical neutrino spectrum for which one wishes to compute the rate. One may then compute the average rate for an ensemble

of events by taking the average, *i.e.*:

$$\Gamma_{\text{tot.}} = \frac{1}{N_{\text{inj.}} \sum_{\text{evts.}} w_{\text{evt.}}}$$

Additionally, we typically define the *oneweight* for an event as:

$$w_{\text{evt.}} = \frac{\Gamma_{\text{evt.}}}{\Phi_{\text{phys.}}(E_{\nu}^{\text{gen.}})}$$

This is a convenient quantity since one may then find the rate for any flux by simply take the product of the flux and the oneweight. Furthermore, this quantity may be used to find the so-called effective area of TAMBO by computing the average value in a given zenith and energy range.

5. Conclusion

TAMBO is a neutrino telescopes that exploits the unique geometry of the Colca valley to detect neutrinos. The unique geometry of TAMBO brings new challenges to neutrino telescopes event generators and simulations. In this contribution, we have introduced the TAMBO simulation framework, which combines existing software for high-energy neutrino propagation, charged tau lepton propagation, and air shower simulation with newly implemented protocols for injecting and weighting neutrino events. This simulation has been orchestrated in the Julia computing language which offers improve performance and ease of use compare to other languages used in particle physics [4].

To the date, all components need to simulate the particle physics processes exist and are currently undergoing validation and injection parameter optimization. This represents a major mile stone in the development of the TAMBO since, once these validation checks have passed, we can begin detail optimization of the detector configuration to further increase the sensitivity of TAMBO to various physical processes. In a future contribution, we will present results using the software describe in this procedure to determine detailed deployment geometries, timing resolution requirements, triggering, and background rejection. Furthermore, we will then be able to present updated sensitivities to various models of the high-energy neutrino flux.

References

- [1] IceCube Collaboration, R. Abbasi *et al.* *Science* **380** (7, 2023) 6652.
- [2] IceCube Collaboration, R. Abbasi *et al.* *Science* **378** no. 6619, (2022) 538–543.
- [3] A. Romero-Wolf *et al.*, “An Andean Deep-Valley Detector for High-Energy Tau Neutrinos,” in *Latin American Strategy Forum for Research Infrastructure*. 2, 2020. [arXiv:2002.06475](https://arxiv.org/abs/2002.06475) [astro-ph.IM].
- [4] J. Eschle *et al.*
- [5] I. Safa, J. Lazar, A. Pizzuto, O. Vasquez, C. A. Argüelles, and J. Vandenbroucke *Comput. Phys. Commun.* **278** (2022) 108422.

- [6] J.-H. Koehne, K. Frantzen, M. Schmitz, T. Fuchs, W. Rhode, D. Chirkin, and J. B. Tjus *Computer Physics Communications* **184** no. 9, (2013) 2070–2090.
- [7] D. Heck, J. Knapp, J. N. Capdevielle, G. Schatz, and T. Thouw.
- [8] **IceCube** Collaboration, R. Abbasi *et al.* *Comput. Phys. Commun.* **266** (2021) 108018.
- [9] F. Halzen and D. Saltzberg *Phys. Rev. Lett.* **81** (1998) 4305–4308.
- [10] A. Garcia, R. Gauld, A. Heijboer, and J. Rojo *JCAP* **09** (2020) 025.
- [11] A. Cooper-Sarkar, P. Mertsch, and S. Sarkar *JHEP* **08** (2011) 042.
- [12] **KM3NeT** Collaboration, A. Garcia and A. Heijboer *PoS ICRC2019* (2020) 895.

Full Author List: TAMBO Collaboration

Jaime Alvarez-Muñiz,¹ Carlos Argüelles², José Bazo³, Jose Bellido⁴, Mauricio Bustamente⁵, Washington Carvalho Jr.⁶, Austion Cummings⁷, Diyaselis Delgado², Pablo Fernández⁸, Alberto Gago³, Alfonso Garcia-Soto², Ali Kheirandish^{9,10}, Jeffrey Lazar^{2,11}, Andrés Romero-Wolf¹², Ibrahim Safa¹³, Harm Schoorlemmer¹⁴, William G. Thompson², Aaron Vincent^{15,16,17}, Stephanie Wissel⁷, Enrique Zas¹, and Pavel Zhelnin²

¹Departamento de Física de Partículas & Instituto Galego de Física de Altas Enerxías, Univ. de Santiago de Compostela, Santiago de Compostela, Spain

²Department of Physics and Laboratory for Particle Physics and Cosmology, Harvard University, Cambridge, MA 02138, USA

³Pontificia Universidad Católica del Perú, Lima, Perú

⁴University of Adelaide, Adelaide, SA, Australia

⁵Niels Bohr International Academy & DARK, Niels Bohr Institute, University of Copenhagen

⁶Departamento de Física, Universidade de São Paulo, São Paulo, Brazil

⁷Department of Physics, Department of Astronomy and Astrophysics, Institute for Gravitation and the Cosmos, Pennsylvania State University, State College, PA 16801

⁸Donostia International Physics Center DIPIC, San Sebastián/Donostia, E-20018, Spain

⁹Department of Physics & Astronomy, University of Nevada, Las Vegas, NV, 89154, USA

¹⁰Nevada Center for Astrophysics, University of Nevada, Las Vegas, NV 89154, USA

¹¹Dept. of Physics and Wisconsin IceCube Particle Astrophysics Center, University of Wisconsin–Madison, Madison, WI 53706, USA

¹²Jet Propulsion Laboratory, California Institute of Technology

¹³Columbia University, New York, NY, 10027, USA

¹⁴Max-Planck-Institut für Kernphysik, Heidelberg, Germany

¹⁵Department of Physics, Engineering Physics and Astronomy, Queen's University, Kingston, ON K7L 3N6, Canada

¹⁶Arthur B. McDonald Canadian Astroparticle Physics Research Institute, Kingston, ON K7L 3N6, Canada

¹⁷Perimeter Institute for Theoretical Physics, Waterloo, ON N2L 2Y5, Canada